Front. Phys., 2012, 7(4): 418–423
DOI 10.1107/s11467-011-0230-z

RESEARCH ARTICLE

Broadband ferromagnetic resonance studies on influence of interface bonding on magnetoeletric effects in ferrite–ferroelectric composites

D. V. B. Murthy*, Gopalan Srinivasan†

Physics Department, Oakland University, Rochester, MI 48309, USA
*E-mail: *murthydvb@ieee.org, †srinivas@oakland.edu*
Received October 18, 2011; accepted November 22, 2011

A systematic study has been carried out on the effects of interface bonding on the strain mediated magnetoelectric (ME) coupling in ferromagnetic–ferroelectric bilayers. The technique used involves the static electric field E tuning of the ferromagnetic resonance (FMR) in yttrium iron garnet (YIG) and lead zirconate titanate (PZT) or lead magnesium niobate-lead titanate (PMN-PT). A broad band detection technique has been developed for studies over 1–40 GHz in three types of bilayers: epoxy bonded, eutectic bonded and YIG films directly grown onto piezoelectric substrate by electrophoretic deposition. The strength A of the converse ME effect (CME) defined as the ratio of the frequency shift δf in FMR in E, $A = \delta f/E$, varies over the range 0.8 to 4.3 MHz·cm/kV, and is the highest for eutectic bonded samples and is the weakest for epoxy bonded bilayers. The results presented here as of importance for dual electric and magnetic field tunable ferrite–ferroelectric microwave resonators and filters.

Keywords ferrite, ferroelectric, magnetoelectric, ferromagnetic resonance

PACS numbers 75.85.+t, 85.80.Jm, 75.50.Gg, 77.84.-s

1 Introduction

Multiferroics with two or more ferroic (ferroelectric, ferroeleastic, ferro/ferri/anti-ferromagnetic) orderings have attracted considerable interests in recent years [1–7]. Single-phase multiferroics are rare and their magnetoelectric (ME) responses are either weak or occur at temperatures too low for practical applications. Ferromagnetic-piezoelectric composites, however, show strong ME coupling at ambient temperatures. The ME effect here is a product-property mediated by elastic deformation [2–5]. The ME phenomena of importance are giant low-frequency interactions and coupling when the electric and/or the magnetic subsystems show resonance, including elelctro–mechanical resonance (EMR), ferromagnetic resonance (FMR) and magneto–acoustic resonance at the overlap of EMR and FMR. Potential device applications for the composites are magnetic field sensors, dual electric and magnetic field tunable microwave and millimeter wave devices, and miniature antennas [3–7].

Magnetoelectric interactions in ferrite–ferroelectric composites, in particular, have facilitated a new class of FMR-based microwave signal processing devices [8–11]. These devices mainly depend on either hybrid spin electromagnetic waves [9, 10] or mechanical force mediated magnetoelectric (ME) interactions [11]. Microwave cavities or stripline structures are conventionally used for measuring the FMR and ME coupling strength in ferrite ferroelectric structures.

Here we focus on two important aspects of ME interactions in ferrite–piezoelectric bilayers: (i) A broad band technique for E-tuning of measurements FMR over 1–40 GHz. (ii) Influence of bonding techniques, i.e., epoxy bonding, eutectic bonding and direct growth of ferrite onto piezoelectric substrates by electrophoretic deposition, on the strength of ME coupling. In this article, we report on a nondestructive and broadband detection of FMR and ME effects resonance in yttrium iron garnet (YIG)-ferroelectric bilayers using a short circuited coaxial electric probe in the frequency range, from 3 GHz to 40 GHz. This paper is organized as follows. Section 2 describes the design of novel near field microwave probe.

The probe consists of a coaxial transmission line connected to a Cu loop which is formed by shorting the inner conductor of a coaxial cable to the outer conductor. Section 3 provides details on bonding techniques. Section 4 provides results of our studies on the strength of ME coupling in YIG-piezoelectric bilayers.

2 A broad-band FMR technique

Several techniques based on scanning probe microscopy (SPM) for imaging spatial distributions of magnetic response in a range of radio frequency (RF), such as electron paramagnetic resonance and FMR, have been developed [12–15]. Toshu *et al.* [16] successfully detected localized FMR signals on a polycrystalline YIG disk and observed strong spatial dependences in detected signal intensities over the sample using open-ended coaxial electric probe. Lee *et al.* [17] demonstrated near field magnetic microscopy by using a shorted coax microwave probe. The shorted microwave probe was designed by soldering the inner and outer conductors of the coax, resulting in a probe that couples magnetically to the sample. Mircea and Clinton [18] extended this technique further by using a thin wire bond to short the coax. This reduced the sample to probe spacing, resulting in an improved electromagnetic coupling. This in turn allowed the use of simpler electronics for the measurements. They also demonstrated the high-bandwidth (40 GHz) FMR probe, where there is no constraint on the sample size or geometry, thus enabling high-frequency measurements on a multitude of materials in their actual operating conditions. Recently microwave resonators based on planar ferrite–piezoelectric structures tuned by magnetic and electric fields have been extensively studied [19, 20]. Nadjib *et al.* demonstrated the electric field induced ferromagnetic shift of $BiFeO_3$–$NiFe_2O_4$ (BFO–NFO) nanocomposites using the shorted microcoax probe [21].

2.1 Design of broad-band FMR probe

A short circuited loop probe, which is made of a coaxial cable with its inner conductor forming a loop shorted with the outer conductor, is designed to directionally enhance the magnetic coupling between the probe and sample, and induce microwave frequency currents of a controlled geometry in the sample.

The probe used in this experiment consists of a SMA connector (Pasternack Enterprises, PE4001) that transmits RF over 40 GHz. The diameter d_1 (d_2) of the outer (inner) conductor of the probe is 5.31(0.6) mm. The outer and inner conductor of the probe is shorted by a Cu–Pt loop. Cu–Pt loops is obtained by sputtering the copper and platinum films of thickness 500 nm and vary in width between 100 μm and 500 μm using the RF Magnetron Sputtering unit. Masks of desired dimensions have been designed to have Cu–Pt loops. The deposition of the platinum over copper film is to have the enhanced sensitivity. The thin film probe design improves the sensitivity of the probe, minimizes the spacing between sample and probe resulting in better coupling and the sheet film geometry generates a highly unidirectional RF field. Figure 1 shows the schematic of the short circuited probe.

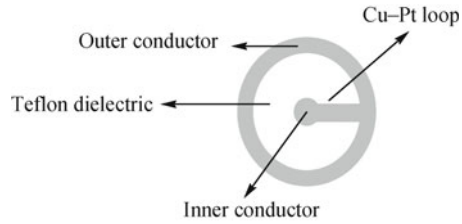

Fig. 1 Schematic of the short circuited microwave coaxial probe for FMR studies over 1–40 GHz.

2.2 FMR studies on single crystal YIG film

The probe was then used for FMR studies on a single crystal film of YIG. A YIG film of thickness of 4 μm and lateral dimensions of 2.2×4 mm^2 was used in measurements. The film was grown by the liquid phase epitaxy on one side of a 0.2-mm-thick gallium gadolinium garnet (GGG) substrate of ⟨111⟩ orientation. The film had a saturation magnetization of 1750 G and a FMR line width of ∼0.6 Oe, measured at 5 GHz. The YIG film was placed on the short circuited coaxial probe, so that the YIG film was in contact with the Cu–Pt loop.

Microwave measurements were carried out using a vector network analyzer PNA-E8361A. A standard calibration procedure for PNA-E8361A was performed before measurements. A CW input signal with $f = 2 - 40$ GHz and power $P_{\text{in}} = 0.1$ mW was applied to the short circuited microwave coaxial probe. Low input power was chosen to prevent heating of the sample due to power absorption at FMR. Profiles of reflected power $P_{\text{ref}}(f)$ vs. f were recorded for a series of H and E. Figure 2 depicts the measured FMR response of the YIG film with bias

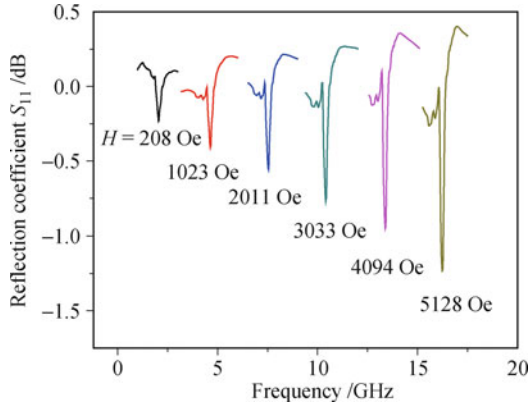

Fig. 2 FMR response of YIG film in the frequency range 3–20 GHz.

magnetic field (H in-plane) from 3 GHz–20 GHz using the microwave probe. Figure 3 shows the FMR response of the YIG film with bias magnetic field (H in-plane) from 20 GHz–40 GHz.

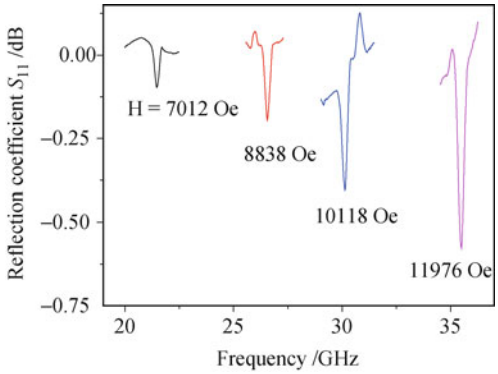

Fig. 3 FMR response of YIG film in the frequency range 20 GHz–40 GHz.

Measured FMR frequency as a function of the bias field is shown in Fig. 4. For a thin YIG film, the FMR frequency f for H perpendicular to the plane is given by

$$f = \gamma(H - 4\pi M) \tag{1}$$

where H is the bias field, $4\pi M$ is the saturation magnetization, and γ is the gyromagnetic ratio. Figure 4 shows a linear dependence over the frequency range $f = 3 - 40$ GHz as expected. Measurements could not be done below 2.5 GHz because of the broadening of FMR due to nonlinear effects.

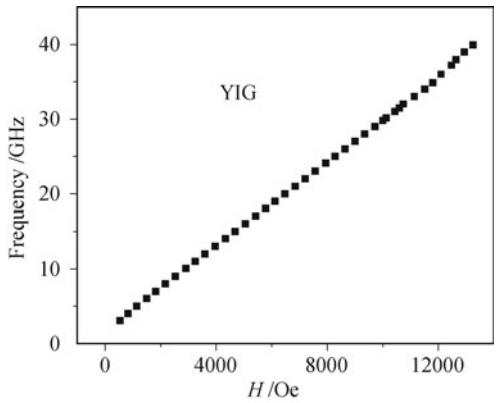

Fig. 4 FMR frequency vs. bias magnetic field for H perpendicular to the plane of YIG film.

3 Bilayer synthesis

For studies on ME coupling polycrystalline $PbZr_{0.52}Ti_{0.48}O_3$ (PZT) or single crystal lead magnesium niobate — lead titanate of the chemical composition 0.68 $[Pb(Mg_{1/3}Nb_{2/3})O_3]$−0.32 $[PbTiO_3]$ (PMN-PT) was used for the piezoelectric phase in the composite. Both the PZT and (001) PMN-PT have high piezoelectric coefficients, large electro–mechanical coupling coefficients, and low dielectric losses [22]. The piezoelectrics, PZT with silver electrodes and PMN-PT with Cr–Au electrodes were initially poled in an electric field. Three different bonding techniques were used: epoxy bonding with a quick dry epoxy, eutectic bonding of YIG and piezoelectric platelet, and growth of YIG film on PZT by electrophoretic deposition (EPD). The bilayer was formed by bonding YIG film to PZT or PMN-PT in the form of 500-μm-thick disk with diameter of 4 mm. The ferrite was bonded to PZT with 2-μm-thick epoxy or by eutectic bonding techniques [23]. For eutectic bonding, a thin layer (100–300 nm) of silicon was deposited onto YIG by RF sputtering and 100-nm-thick silver on PZT or PMN-PT. The bilayer was then placed in a furnace, subjected to a nominal pressure and heated to 600 C. After the high temperature treatment the sample was poled at room temperature. We also grew YIG films on PZT to study ME coupling in a system free of any bonding medium and that is discussed next.

3.1 EPD Growth of YIG on PZT

A bonding medium at the interface is expected to give rise to a significant reduction in the ME effect in ferrite–ferroelectric bilayers. So there is critical need for bilayers obtained by direct deposition of ferromagnetic phase on to a piezoelectric substrate or vice versa. Electrophoretic deposition (EPD) is a powerful tool for the deposition of oxides, metals, and composites [24, 25]. The main advantage of the technique is the ability to control the thickness and morphology of films through simple adjustment of the deposition time and applied potential. Kurinec *et al.* reported the synthesis and EPD deposition of Nickel ferrite nano particles [26]. Hashi *et al.* studied the high frequency characteristics of the Nickel Zinc ferrite film deposited using EPD [27]. Takenaka *et al.* performed the studies on YIG nanoparticle films using inductively coupled RF plasmas [28]. Recently, EPD coating of Mn–Zn ferrites was employed in the fabrication of on-chip inductors [29].

In this work we focused on a layered multiferroic structure obtained by the EPD deposition of YIG films on PZT and (001) PMN-PT. Our interest is in the demonstration of magnetoelectric interactions of these films at microwave frequencies in this unique structure. YIG nano particles synthesized by coprecipitation techniques were used for the deposition of films of thickness 10–100 μm. The bilayer thus obtained was used for microwave ME studies.

The powders of YIG ($Y_3Fe_5O_{12}$) were prepared by the coprecipitation technique by dissolving $Y(NO_3)_36H_2O$ and $Fe(NO_3)_3$, $9H_2O$ with $[Fe^{3+}]/[Y^{3+}] = 5/3$, into an ammoniacal solution of pH = 10. The obtained precipitate was washed several times with deionized water and ethanol, filtered and dried at 65°C for 24 h. The powders were then calcined at 1200°C to form fine garnet

particles.

In EPD, charged powder particles, dispersed or suspended in a liquid medium gets attracted and migrates towards an electrode of opposite charge and consequently gets deposited there under the influence of a DC electric field (electrophoresis), forming a relatively dense and homogeneously compact film. The EPD was performed in a cell with two electrodes vertically immersed in a solvent media. The solvent media [Ethanol (150 mL), PVB (1 mg) and Phosphate Ester] is stirred by magnetic stirrer for 30 min. The pH of the suspension is maintained at 3.5. Then one gram of synthesized YIG nano particles was introduced into the cell. An aluminum plate was used as the anode, and aluminum plate with PZT disc was used as the cathode. They faced each other at a distance of 5 mm. Sedimentation of the particles was prevented by slow stirring using stainless steel mixer which is introduced in the cell. Electrophoretic deposition was carried out for 90 minutes at a constant voltage condition of 25 V. The obtained deposits were dried in air at room temperature. In order to support higher annealing temperatures, Titanium (15 nm)–Platinum (500 nm) are deposited on both sides of the PZT samples. The deposited thin films are annealed at 1050°C.

Figure 5 gives representative data that show the microscope images and structure of the YIG–PZT heterostructure. A 6-μm film was fabricated by EPD at a deposition rate of 400 nm/min. The films were found to be composed of large particles of 150–200 nm size, whereas the size of particles in the starting solution was in the range 10–20 nm. It is considered that the particles undergo agglomeration during deposition.

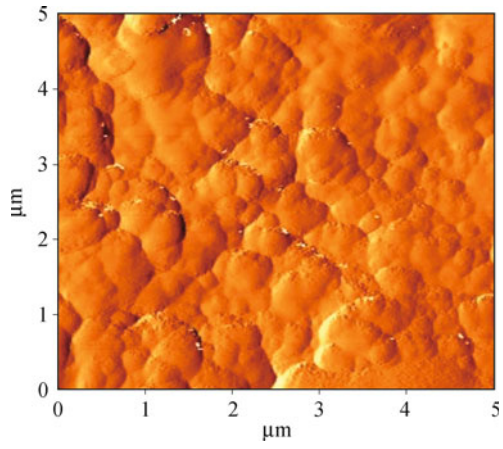

Fig. 5 Atomic force microscopy image of the deposited YIG film on PZT.

4 ME Interactions in YIG-piezoelectric bilayers: Results and discussion

We discuss next static electric field tuning of the FMR in the bilayers for measurements of the converse ME coupling strength. Studies were carried out on epoxy bonded and eutectic bonded bilayers and EPD YIG films on PZT or PMN-PT.

4.1 Epoxy bonded bilayers

The schematics of the YIG-PZT bilayer and the coaxial probe structure are shown in Fig. 6. A PZT plate of dimensions of 4 mm × 4 mm × 0.5 mm and with 5-μm-thick silver electrodes on both sides and was bonded to the YIG film with a fast-dry epoxy. The bilayer was placed on the short circuited coaxial probe, so that the GGG side was in contact with the Cu–Pt loop. The device structure was placed in between the poles of an electromagnet so that a bias magnetic field H is applied perpendicular to the bilayer plane. FMR response of the YIG–PZT bilayer structure is performed. Electric field tuning measurements were performed at frequencies (3–40 GHz) for the YIG–PZT bilayer structure using microwave coaxial probe. A dc electrical field $E = 0 - 10$ kV/cm was generated across PZT by applying a voltage.

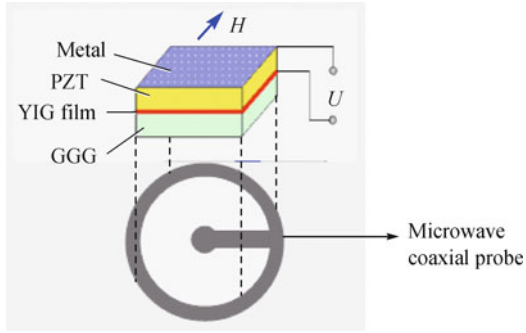

Fig. 6 Diagram showing YIG-PZT bilayer over short circuited microwave coaxial probe.

Figure 7 depicts the E-field tuning characteristics of YIG–PZT structure at 15 GHz. With the application of $E = 1 - 10$ kV/cm, the FMR peak shifted to a higher frequency. The data in Fig. 7 shows a linear increase in δf with H and an ME coefficient $A = \delta f/E \approx 1$ MHz·cm/kV. When the polarity of E was reversed by reversing the voltage applied to PZT, the peak downshifted by $\delta f = -14$ MHz for $E = 10$ kV/cm. It is seen that average shift is in the range of 1.8 MHz for

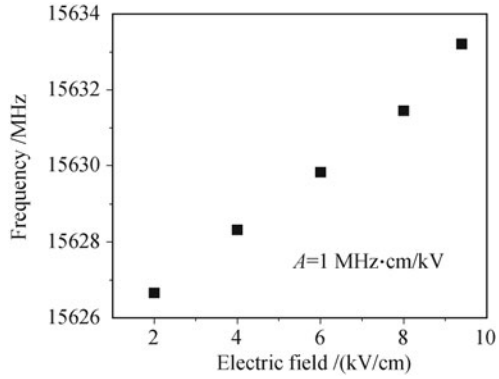

Fig. 7 E-field tuning characteristics for epoxy bonded YIG-PZT bilayer.

$E = 1$ kV/cm, for H orientation (out of plane).The observed shift arises due to magnetoelectric interactions. Application of E to PZT brings about a compressive or tensile strain, depending on the direction of E, resulting in a deformation of the YIG film, leading to a change in the internal magnetic field. The range of frequency tuning could potentially be increased by decreasing thickness of the GGG substrate or with the use of stronger piezoelectrics than PZT.

In the similar manner, bilayer (2 mm × 2 mm) were fabricated with 4-μm-thick epitaxial (111) YIG films on GGG substrate and 0.5-mm-thick (001) PMN-PT. Gold electrodes (0.2 μm) were deposited on PMN-PT for electrical contacts. A thin layer (< 0.08 mm) of an epoxy (ethyl cyanoacrylate) was used to bond YIG. Initially, FMR response of the YIG/PMN-PT bilayer structure was studied. E-field tuning measurements were performed at various frequencies from 3–40 GHz using the microwave coaxial probe. Figures 8 and 9 show the dependence of the frequency shifts δf on E at frequencies $f = 20$ GHz and 35 GHz, respectively. The estimated $A = \delta H/E \approx 3.2$ and 4.7 MHz·cm/kV, respectively, for 20 GHz and 35 GHz. The ME coefficients for epoxy bonded samples are in agreement with previous reported values for epoxy bonded samples [30].

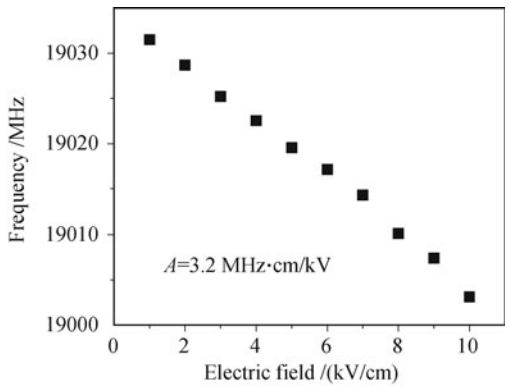

Fig. 8 E-field tuning characteristics of FMR for epoxy bonded YIG-PMN-PT at 20 GHz.

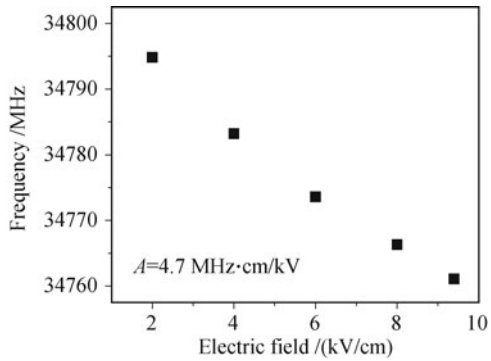

Fig. 9 Data as in Fig. 8 for YIG/PMN-PT at 35 GHz.

4.2 ME effects in eutectic bonded samples

Similar ME measurements were performed on eutectic bonded bilayers. Samples were bonded with 100 nm silver on PZT and 100–500-nm-thick Si on YIG. Figure 10 shows E-tuning data on δf vs. E for a bilayer in which the Si layer was 100 nm in thickness. The ME coefficient A estimated form the data is 2.2 MHz·cm/kV which is a factor of 2 higher than for epoxy bonded for YIG-PZT (Fig. 7). Samples with 300- and 500-nm-thick Si layer bonding were studied and estimated A vs. thickness of Si is shown in Fig. 11. One observes a linear decrease in A with increasing thickness of Si. Thus the eutectic bonding shows a critical dependence on Si thickness with A falling rapidly to values below the A for epoxy bonding when Si thickness exceeds 300 nm.

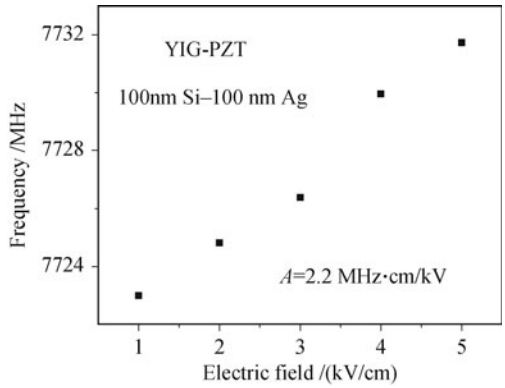

Fig. 10 E-tuning of FMR in eutectic bonded YIG-PZT.

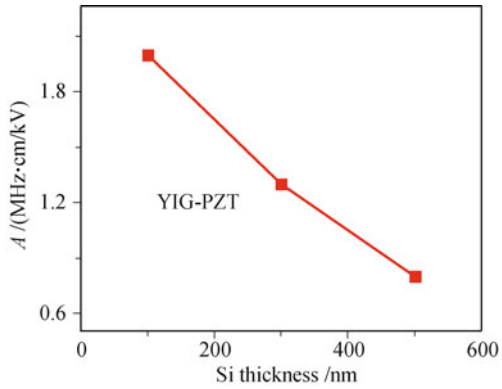

Fig. 11 ME coefficient A vs. thickness of Si in eutectic bonded YIG-PZT.

4.3 ME coupling in EPD films of YIG on PZT

Microwave measurements were performed on EPD deposited YIG films over PZT samples to study the behavior of ferromagnetic resonance, effective line width and electric field tunable characteristics. Figure 12 depicts the reflection coefficient of the YIG film deposited on PZT sample for 90 minutes for static field $H = 340$ Gauss. For $E = 0$, the spectrum contained a well defined FMR absorption peak with a central frequency $f = 1.76$ GHz, a maximum absorption of 3.5 dB and a 3 dB linewidth $\Delta f = 282$ MHz. With the application of $E = 10$ kV/cm FMR up-shifted by $\delta f = 12$ MHz, corresponding to $A = 1.2$ MHz·cm/kV. When the polarity of E was

changed by reversing the voltage applied to PZT, the peak is downshifted by 12 MHz. Similarly the electrical tuning characteristics of the deposited YIG films on the PZT resonator for 60 and 120 minutes were performed. The maximum tuning range is 14 MHz and 6 MHz, respectively, for 60 and 120 minutes at $E = 10$ kV/cm. It is clearly observed that with increase in the deposition time, shift in the FMR frequency of YIG film decreases due to the applied E-field over PZT sample. In the same manner EPD deposition of YIG films were carried out on PMN-PT sample for 90 minutes. The FMR response shows a shift of about 25 MHz as one applies 10 kV/cm across the ferroelectric PMN-PT layer that corresponds to $A = 2.5$ MHz·cm/kV at 4 GHz.

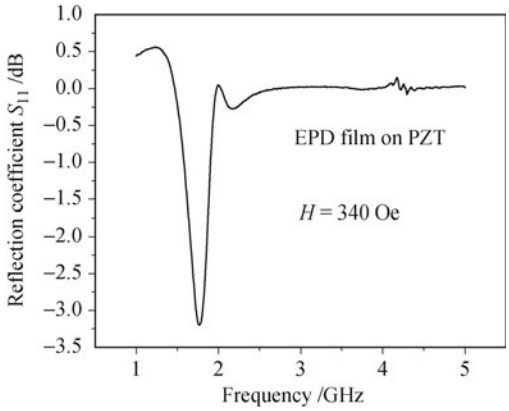

Fig. 12 Reflection coefficient S_{11} vs. f profile showing FMR in EPD YIG film on PZT substrate.

5 Conclusions

We used a versatile technique to characterize the ferromagnetic resonance (FMR) and magnetoelectric effects at ferromagnetic resonance in ferrite ferroelectric microwave structure using a short circuited coaxial probe. The technique has sensitivity comparable to that of well-established methods besides its non-contact nature, broadband and local. We measured FMR response of the YIG film as a function of frequency and the resonance frequency vs. H data showed the expected linear variation for H perpendicular to sample plane. The broadband technique and the traditional stripline technique were used to measure the strength of ME coupling in bilayers of YIG and PZT or PMN-PT. Bilayers made by epoxy bonding and eutectic bonding of YIG to piezoelectric platelets and YIG film deposited by electrophoretic deposition on PZT or PMN-PT were studied. For a specific thickness of YIG, Si–Ag eutectic bonded samples show the highest ME coupling coefficient only when the thickness of Si and Ag is around 100 nm. For higher thickness of Si, A decreases to values measured for epoxy bonded or YIG films grown on PZT.

Acknowledgements The research was supported by a grant from the Office of Naval Research.

References

1. M. Fiebig and N. A. Spaldin, Eur. Phys. J. B, 2009, 71: 293
2. K. F. Wang, J. M. Liu, and Z. F. Ren, Adv. Phys., 2009, 58: 321
3. C. W. Nan, M. I. Bichurin, S. X. Dong, D. Viehland, and G. Srinivasan, J. Appl. Phys., 2008, 103: 031101
4. R. Ramesh and N. A. Spaldin, Nat. Mater., 2007, 6: 21
5. M. Vopsaroiu, J. Blackburn, and M. G. Cain, J. Phys. D, 2007, 40: 5027
6. G. Srinivasan, Ann. Rev. Mater. Res., 2010, 40: 153
7. G. Lawes and G. Srinivasan, J. Phys. D, 2011, 44: 243001
8. M. I. Bichurin, R. V. Petrov, and Yu. V. Kiliba, Ferroelectrics, 1997, 204: 311
9. W. J. Kim, W. Chang, S. B. Qadri, H. D. Wu, J. M. Pond, S. W. Kirchoefer, H. S. Newman, D. B. Chrisey, and J. S. Horwitz, Appl. Phys. A, 2000, 71: 7
10. A. A. Semenov, S. F. Karmanenko, B. A. Kalinikos, G. Srinivasan, A. N. Slavin, and J. V. Mantese, Elec. Lett., 2006, 42: 641
11. G. Srinivasan and K.Y. Fetisov, Ferroelectrics, 2006, 342: 65
12. K. R. Smith, M. J. Kabatek, P. Krivosik, and M. Wu, J. Appl. Phys., 2008, 104: 043911
13. D. Rugar, R. Budakian, H. J. Mamin, and B. W Chui, Nature, 2004, 430: 329
14. R. Meckenstock, Rev. Sci. Instrum., 2008, 79: 041101
15. Y. Obukhov, D. V. Pelekhov, J. Kim, P. Banerjee, I. Martin, E. Nazaretski, R. Movshovich, S. An, T. J. Gramila, S. Batra, and P. C. Hammel, Phys. Rev. Lett., 2008, 100: 197601
16. T. An, N. Ohnishi, T. Eguchi, Y. Hasegawa, and P. Kabos, IEEE Magn. Lett., 2010, 1: 3500104
17. S. C. Lee, C. P. Vlahacos, B. J. Feenstra, A. S. Schwartz, D. E. Steinhauer, F. C. Wellstood, and S. M. Anlage, Appl. Phys. Lett., 2000, 77: 4404
18. D. I. Mircea and T. W. Clinton, Appl. Phys. Lett., 2007, 90: 142504
19. Y. K. Fetisov and G. Srinivasan, Appl. Phys. Lett., 2006, 88, 143: 503
20. A. B. Ustinov, Yu. K. Fetisov, and G. Srinivasan, Tech. Phys. Lett., 2008, 34: 593
21. N. Benatmane, S. P. Crane, F. Zavaliche, R. Ramesh, and T. W. Clinton, Appl. Phys. Lett., 2010, 96: 082503
22. L. E. Cross, in: Ferroelectric Ceramics: Tailoring Properties for Specific Applications, Ferroelectric Ceramics, edited by N. Setter, Basel: Birkhäuser, 1993
23. Y. G. Li, J. Sun, C. S. Yang, J. Q. Liu, S. Susumu, and T. Katsuhiko, Chin. Phys. Lett., 2011, 28(6): 068103
24. O.O. Van der Biest, L. J. Vandeperre, Annu. Rev. Mater. Sci., 1999, 29: 327
25. I. Zhitomirsky, Advances in Colloid and Interface Science, 2002, 97: 279
26. S. K. Kurinec, N. Okeke, S. K. Gupta, H. Zhang, and T. D. Xiao, J. Mater. Sci., 2006, 41: 8181
27. S. Hashi, S. Yabukami, A. Maeda, N. Takada, S. Yanase, and Y. Okazaki, J. Mag. Magn. Mater., 2007, 316: 465
28. K. Takenaka, H. Nakayama, Y. Setsuhara, H. Abe, and K. Nogi, Surface and Coatings Tech., 2008, 202: 5336
29. C. Washburn, D. Brown, J. Cabacungan, J. Venkataraman, and S. K. Kurinec, Materials Research Society Symposium Proceedings: Materials, Integration and Technology for Monolithic Instruments, 2005, 869: 157
30. S. Shastry, G. Srinivasan, M. I. Bichurin, V. M. Petrov, and A. S. Tatarenko, Phys. Rev. B, 2004, 70: 064416